International Journal of Scientific Research in Multidisciplinary Studies
Vol.5, Issue.9, pp.15-22, September (2019)

Research Paper
E-ISSN: 2454-9312
P-ISSN: 2454-6143

Parametric Analysis of Centrifugal Pump and Calculation of Slip Factor

Jogendra Kumar[1*], Maksudan Paswan[2]

[1,2]Mechanical Engineering, Madan Mohan Malaviya University of Technology, Gorakhpur, India

[*]*Corresponding Author: jkmmmut@gmail.com, Tel.: +919653011169*

Available online at: www.isroset.org

Received: 25/Aug/2019, Accepted: 20/Sept/2019, Online: 30/Sept/2019

***Abstract*—**Centrifugal pumps are one of the turbomachines mostly used in different industries. The current research aims to determine the pump's best working condition, where it must be run at minimum energy input with the optimum effectiveness, using a numerical technique such as computational fluid dynamics. The whole test (CFD) is performed using the commercial software ANSYS CFX 15.0. ANSYS CPD with a 22.5 ° angle of outlet blade and 6 sets of blades produced the pump's geometry. The current assessment has shown that the pump's effectiveness is reduced as the mass flow rate is increased. A second parameter, like the centrifugal pump slip factor, is calculated. The average slip factor calculation value is 0.83, the highest value for calculating the slip-factor in the Wisner analytical model.

Keywords—Computational fluid Dynamics, ANSYS CFX, Vista CPD, Mass flow Rate, Pump

I. INTRODUCTION

Centrifugal pumps are roto-dynamic presses which pressure liquids to the required height at the required flow rate. The name of the roto-dynamic portion comes from a centrifugal pump impeller. The most widely used rotating pump types, which represent 25% of total electricity, are centrifugal pumps. The centrifugal pump impeller is powered by external primary movers, such as electric motors, steam-engines, etc. In almost all sectors, centrifugal pumps have a lot of apps. Due to the high speed of the design and performance analysis of the centrifugal pump, the job is extremely challenging [1]. The performance of the centrifugal pump depends on a number of parameters, including the number of blades, the blade angle at the end of the impeller's exit (a rotating part). Centrifugal pump primarily has two components namely (a) an impeller forced by impeller action to make the liquid circulate, (b) a pump box, forced into the impeller by rising to elevated pressure. A primary electrical motor drives the rotor installed on a shaft. The pump box contains the suction and discharge tube and is mounted in the rotor. The liquid is sucked through the suction pipe and the impeller vanes bring it into circular motion. The rotating channel is formed by the rods and side walls and ropes. The liquid is produced at very elevated pressure and velocity at the outlet rather than at the entrance of the impeller. The pump casing shifts partially in the form of pressure before the pump leaves the pump via the discharge [3]. There are plenty of cash and time spent on centrifugal pump design and analysis. This decreases the pumping industry's profit. The CFD method is used to solve this issue before the centrifuge pump is finally manufactured. CFD technology can provide what's going on inside the turbomachines. The centrifugal pump effectiveness relies on centrifugal pump geometry and working condition, multiple blades, slip factor, etc. [4]. Pressure at the impeller's eye inlet, mass flow rate through the pump, head at which water must discharge, may be the working situation. The blade angle at the pump outlet [5].

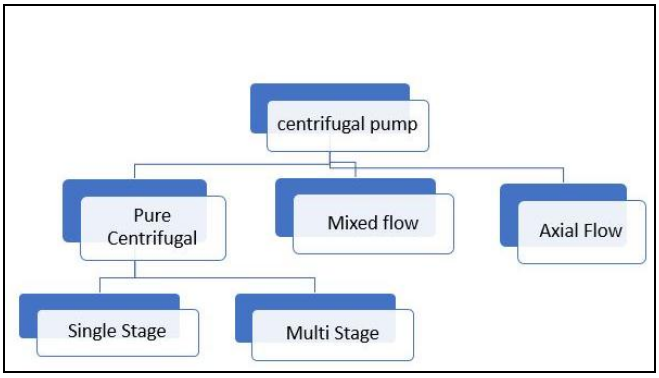

Figure 1. Classification of Centrifugal Pump

In radial turbo, slip phenomenon occurs. As the impeller passage flows, there is a distinction in pressure and velocity between the impeller blades ' leading and trailing faces [2]. On the leading face of a blade, there is relatively high pressure and low velocity, while on the trailing face, the

pressure is higher, and velocity is higher. This results in the circulation around the blade and non-uniform velocity distribution at any radius [6]. Due to this tangential component of velocity gets Reduced and therefore decreased energy provided by the impeller. In a radial centrifugal pump, different parameters influence the slip phenomenon such as volume flow rate, outlet blade angle, number of blades, type of liquid (water, oil, etc.) [7]. F.J Wiesner and others. 8] suggested a review paper on the various slip factor calculation trends and study fields for impellers. The general comparison of prior job introduces Baseman's job, who gave the empirical relationship for calculating the slip factor based on geometric parameters such as multiple blades, internal and outer blade radius, etc. The relationship is also provided for pumps that exceed the restricting percentage of the radius. The tabular information is summarized in the final contact as the slip factor for 60 pumps with test information outcomes and the writer specifies a few more outcomes. Weidong Zhou et. al. [9] worked with the three constructed centrifugal pumps and conducted flow pattern computational fluid research. They intended three distinct pumps with 4 straight blades and 6 twisted type blades and used Naiver-Stokes momentum conservation equations to perform CFX simulation. They evaluated the distribution of pressure and velocity in all three pumps using this solver. In the simulation, they discovered that the outcome of straight blade pumps was somewhat distinguished, but the outcomes for both twisted blades were shown to be better than the straight blade centrifugal pumps. Jose A Caridad et. al. [10] simulated both single and two-phase centrifugal impellers using a CFD tool. For the research, the impeller's computing domain is taken with regard to analyse experimental job with the particular 1960 velocity along with the liquid flow rate, bubble diameter and gas void fraction being regarded as independent variables. The 2-phase fluid is used with the k-e turbulence model. Simultaneously repeated the operation for single-phase fluid testing for 4 more pump designs at distinct speeds. The findings achieved are contrasted with that of analyse with distinct gas void fraction 0 (single phase), 10%, and 15% and discovered the notable agreement and proposed that slip factor is significant phenomena and there is more to look up with two-phase flows and impeller efficiency. Memardezfouli and Mohamad.et. al. [11] contributed their job by using experimental job to estimate the slip factor. They researched the industry's five centrifugal pump and attempted to figure out the slip variables based on previous research empirical relationships and estimated the circumstances slip factor. They also discovered a function of outlet velocity to be the slip factor. Finally, they extracted some relationships with considering the slip factor off-design calculation and suggested the slip factor assessment data table straight from the centrifugal pump geometric parameter. B. Jafarzadeh et al [1] operate on the flow phenomena in a centrifugal pump using CFD models of fluent turbulence. Consideration was given to the pump of three distinct blade number (5,6,7) and simulation was conducted on separate blade pumps with all three kinds of turbulence modelling method and ideal model was chosen from the three. RNG k-e model achieved the best outcomes and convergence. They also conducted a pump effectiveness inquiry and discovered that the 7-blade pump showed optimum outcomes and concluded that the volute casing position of the blade tongue could cause flow separation [12]. Yanxia Fu et. al. [6] in (2014) research included cavitation phenomena and low flow stability issues. They conducted the impeller's CFD analysis for distinct flow rates and discovered the drop-in vapor drop resulting in the flow pattern being unstable. They conducted the experimental study on the same configuration pump type with corresponding flow rates as mentioned in numerical simulation [13] for in-depth knowledge. They used large frame movie cameras and configuration with elevated frame rates because of quick and unstable flow. The flow pattern was researched and excellent agreement with the numerical outcomes was shown in the outcomes acquired. Mohamed G Khalafallah et al [11] studied the slip phenomenon and reliance on the flow rate of the four-bladed centrifugal pump. Their research involves frozen-other method and rotationally periodic boundary conditions. They discovered that the pump output was useful with a 4 percent relative error and a flow coefficient within 0.8-1.2[14]. In addition, the calculated slip factor value, which is the flow rate function, is validated with Qui's slip factor calculation mathematical model as F=0.52. They discovered that raising the number of blades for pump to 10 gives up to 0.69 in slip factor saturation along with a rise of 30 percent-50 percent in splitter improves the slip factor [15]. Therefore, by magnifying the number of splitters, they achieved the sum of 1 hydraulic effectiveness around the value. M. Lorusso et. al. [16] The article examines the impact of coarser mesh elements on the NPSH assessment and the Centrifugal Pump head. It is discovered that the coarse mesh has little impact on the NPSH value and has a greater impact on the pump-developed head. Sunil R. Patil et. al. [17] The results were as the clearance of the tongue reduced the pump effectiveness. The effectiveness and pressure increase respectively risen to 21.90 percent to 19.52 percent at the complete release. T. Capurso et. A double suction centrifugal pump impeller with a specified velocity of less than 60 was intended. Open Foam CFD software analyses the results. The model k-r SST is used to capture the turbulence in the region of the passage of the impeller. It was discovered that the effectiveness was enhanced by embracing the fresh navel impeller layout (1-2 percent) compared to the standard modelling H. et. al. [18] chosen five distinct models of impellers with distinct outlet blade angles such as 230, 250, 270, 290 and 310. An experiment was conducted to evaluate the centrifugal pump based on variable outlet blade angle and it was found that the pump head increased with the rise in the outlet blade angle [19].

We can conclude from the above literature that the slip phenomenon is the most significant parameter in the Centrifugal pump efficiency assessment [20]. The pump's distinctive curve is called the head created by the pump with mass flow rate through the pump at a pump's static velocity. The pump, effective and shaft power with velocity, result in the variation in the head following a definite rule known as affinity legislation.
Head developed by the pump.

$$H = mass\ flow\ avg\ \frac{(P_{t,out} - P_{t,inlet})}{\rho g} \quad (1)$$

Where Pt, out = Total pressure at the outlet of the pump, Pt, inlet = Total pressure at the outlet of the pump, ρ = Density of the water, g= gravitational acceleration[6].

The Torque required by the pump.

$$T_{shaft} = \int_{r_1}^{r_2} [(r \times n).p + (r \times \tau_w) cot\beta_2'] b.dr \quad (2)$$

Shaft power, P_{shaft}

$$P_{shaft} = T_{shaft} * \omega \quad (3)$$

Where ω = angular velocity of the impeller.
Power developed by the Pump

$$P_{pump} = \dot{m} g H \quad (4)$$

Where $\dot{m}$ = Mass flow rate through the Pump, H = Head developed by the Pump.
Total efficiency

$$\eta_t = \frac{P_{pump}}{P_{shaft}} \quad (5)$$

η_t = Total Efficiency of Pump, P_{pump} = Power developed by the Pump
The Mass Flow Rate through the Pump

$$\dot{m} = \pi D_2 b_2 C_{m_2} \quad (6)$$

D_2 = diametre of the impeller
Head variation with a Mass Flow Rate

$$H = A - B\dot{m}cot\beta_2' \text{ [21]} \quad (7)$$

A and B are the constants, $\dot{m}$ = Mass Flow Rate, β_2' = Outlet Blade Angle.

II. METHODOLOGY

The pump efficiency and slip factor are calculated using the computational fluid dynamics. Under the specified block diagram, CFD technology is research as shown below [22]. The method performs effectively and follows the route.

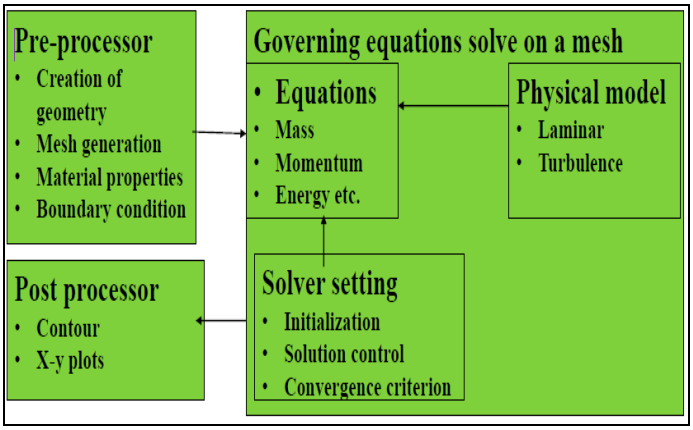

Figure 2. Framework of CFD Simulation

A Centrifugal Pump's design The original phase of CFD simulation is the development of the flow area design also known as the computing domain. ANSYS vista CPD (Centrifugal Pump Design) creates the geometry of the centrifugal pump in this research.

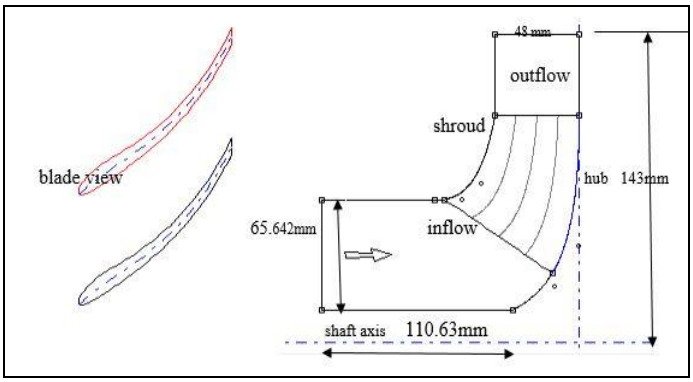

Figure 3. Meridional View of Impeller Passage

A. *Impeller Design Parameters*

Table 1. Design Parameters of Impeller and Blade

s.no.	Impeller angle	Impeller outlet	Exit width(b)
1	$\alpha_1 = 90°$	$\alpha_2 = 11.11°$	48.6mm
2	$\beta_1' = 16.44°$	$\beta_2' = 22.4°$	Z=6

z = Number of Blades β_1' = inlet Blade Angle, β_2' = outlet Blade Angle, α_2 = Outlet Flow Angle[23].

Shroud is the plate where the blades are connected to which mechanical resistance is provided. It guides the liquid and prevents the axis of the shaft from coming out of the liquid. Hub can be described as the base plate that casts blades on. Depending on our demands, pump impeller can be used with hub less. It is possible to use impeller with hub for the fluid with suspended particles. Usually used for pumping transparent fluids when the impeller has both a shroud and a hub. Less thrust experiences the impeller being closed

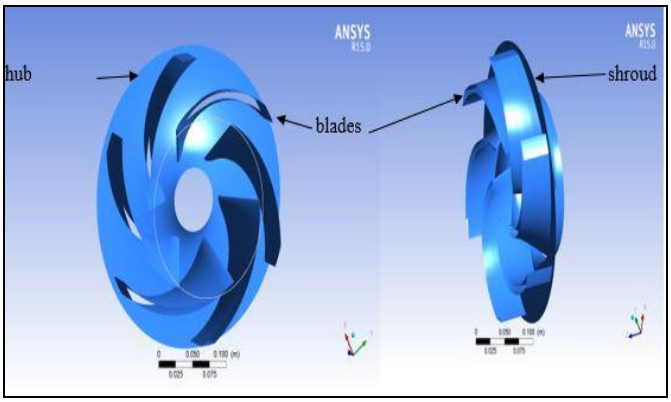

Figure 4. Impeller Blade, Hub and Shroud

B. Volute Geometry

Liquid discharge in volute arises from the impeller. The volute's shape is like a spiral. The minimum is where liquid discharge is referred to as the tongue and rises gradually along the exit plane. The case reflects the volute inlet diameter.

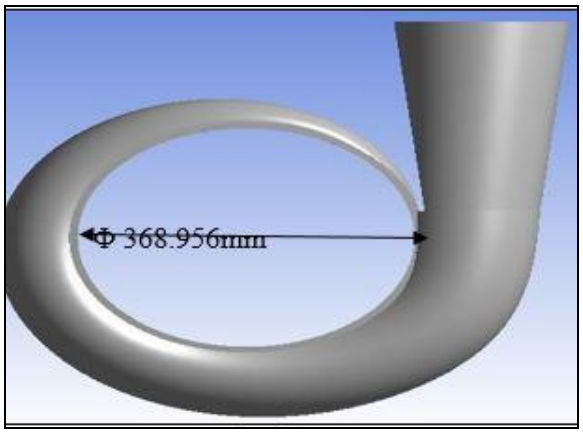

Figure 5. Volute of Centrifugal Pump

C. The meshing of Impeller Domain and Volute Domain:

It is known as mesh to divide the computing domain into several subdivisions into tiny rectangular and trigonal components. We fix the discrete value of the flow variable like velocity, pressure temperature in the computation domain. The solution's precision relies on how well the mesh was created. The quality of the mesh being produced is defined by different parameters. Skewness and the mesh elements ' orthogonal performance. Near-zero skewness is a decent quality mesh, and near-1 orthogonal quality is the highest quality mesh. ANSYS Terbogrel meshed the impeller domain. ANSYS Turbo Grid is intended specifically for turbomachinery meshing. The complete size of the mesh impeller and a nearer view of the mesh near the blade region are shown in Figure 6. In the figure, around the blade passage, we can see beautiful hexahedral mesh.

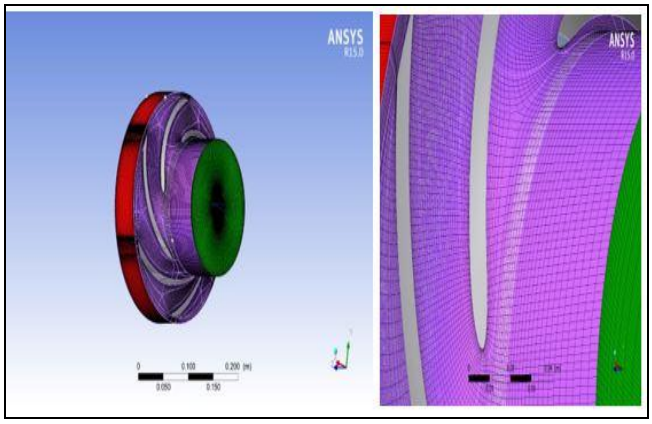

Figure 6. Structured Mesh near Impeller Blade

The meshing of a centrifugal pump is performed with an average skewness value of 0.2641 in ANSYS Mesher version 15.0. The complete number of components is calculated in 191345. The value of skewness is used to check the quality of the mesh components.

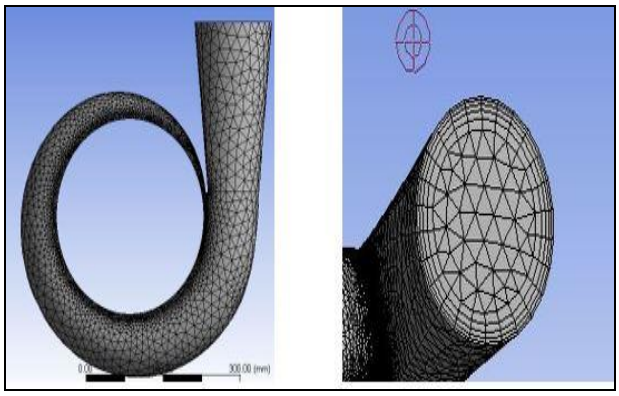

Figure 7. Meshing of volute Domain

Table 2. Details of Elements

No. of.	Coarser mesh	Medium mesh	Fine mesh	Very fine mesh
elements	299499	419294	646655	854200

We change the number of elements of the meshed geometry for mesh-independent test figure 3.16 and select a parameter to vary with regard to mesh size. For the mesh convergence test, the head created by the pump is chosen here. It is found that the head converges at an element size of 646655 to the

positive value of 16 m and it does not change much regarding the enhanced number of components in the geometry. We will have a solution in this no. of components that is not dependent on the mesh size. The error that triggered the meshing of the components is called the error of truncation that minimizes as we reduce the size of the component.

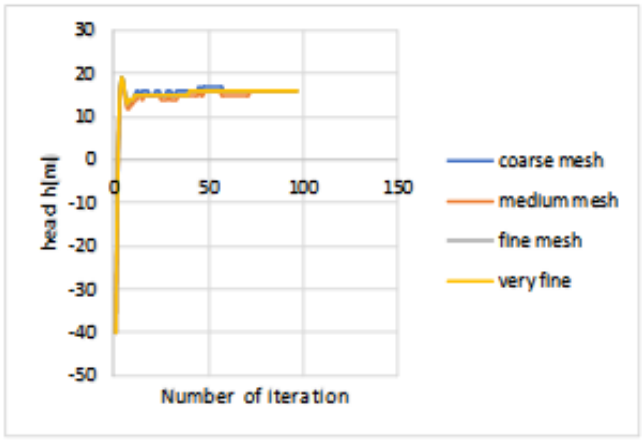

Figure 8. Mesh independence Test

Water is used as the 1000-density working liquid (kg / m^3). It is presumed that water is the incompressible liquid with a dynamic viscosity of $\mu = 8.9 \times 10^{-4} \frac{kg}{sec^2}$. The absolute zero pressure and complete m of 77.8 kg / sec is used as the volute reservoir at the centrifugal pump inlet. Since the impeller is modeled in the reference rotating frame, hub, the impeller rotates the shroud. There is no slip situation on the hub's rotating walls and the impeller's shroud and blades. No slip condition on the walls indicates the relative velocity of the fluid particle adhering to the shroud walls and the hub is zero.

III. GOVERNING EQUATION

Based on the diameter of the impeller of the diameter of Impeller the Reynolds number is calculated as 29.52×10^5.

$$Re_D = \frac{\rho \bar{U} D}{\mu}$$

$\rho = 1000\ kg/m^3$,
$\bar{U} = average\ velocity\ at\ the\ inlet\ at\ the\ inlet = 9.19\ m/sec$

$$D\ diameter\ of\ the\ impeller = 28.6\ cm$$
$$\mu = 8.9 * 10^{-4}\ kg/\sec^2$$

Based on the Reynolds number turbulence model, flow factors such as stress, velocity elements are chosen for calculation. The governing equations here are mass and momentum conservation and are solved on the components on each mesh. In the rotating zone, the volute domain is modeled and the volute in the stationary zone.
Continuity equation in 3D

$$\frac{\partial \rho}{\partial t} + \frac{\partial (\rho u_i)}{\partial x_i} = 0 \qquad (8)$$

u_i = Velocity in ith direction, where i = 1,2,3 x_i = Co-ordinate direction
u_1 = Velocity in x direction, u_2 = Velocity in y direction, u_3 = Velocity in z direction
x_1 = x direction, x_2 = y direction, x_3 = z direction
The governing equations are the Naiver-Stokes Equation (14) that captures the flow variables in the fluid flow.

$$\rho \frac{\partial u_i}{\partial t} + \rho u_j \frac{\partial u_i}{\partial x_j} = -\frac{\partial p}{\partial x_i} + \frac{\partial \tau_{ij}}{\partial x_i} - \rho[2\omega \times u_i + \omega \times (r \times \omega\ )] \qquad (9)$$

τ_{ij} = shear stress in the fluid layers, r = position vector with respect to origin.

$$\tau_{ij} = 2\mu \delta_{ij}\ \delta_{ij} \qquad (10)$$

$$\delta_{ij} = \frac{1}{2}\left(\frac{\partial u_i}{\partial x_j} + \frac{\partial u_j}{\partial x_i}\right) \qquad (11)$$

δ_{ij} = Shear Stress Tensor. ω = Constant Angular Velocity of the Fluid
If the flow is turbulent each flow variable can be decomposed into mean and fluctuating part. Putting $u_i = \bar{u} + u_i'$ and $p = \bar{p} + p_i'$, in equation (14), neglecting body forces we get Reynolds Average Naiver-Stokes (RANS) equation (17). RANS equation governs the mean of the flow.

$$\rho \overline{u_j} \frac{\partial \bar{u}_i}{\partial x_j} = \frac{\partial}{\partial x_i}\left[-\bar{p}\delta_{ij} + \mu\left(\frac{\partial \bar{u}_i}{\partial x_j} + \frac{\partial \bar{u}_j}{\partial x_j}\right) - \overline{\rho u_i' u_j'} - \rho[2\omega \times \bar{u}_i + \omega \times (r \times \omega\ )]\right] \qquad (12)$$

$\bar{u} = Mean\ Velocity, u_i'$ = Velocity fluctuation, $\overline{\rho u_j' u_j'}$ = Reynolds Stress.
$\bar{u} = Mean\ Velocity, u_i'$ = Velocity fluctuation, $\overline{\rho u_j' u_j'}$ = Reynolds Stress.
The Reynolds stress contains additional six unknowns. The equation (17) can be solved if we relate Reynolds Stresses with mean quantities. In (1868) Bossiness' Linked Reynolds stresses to the mean rates of deformation.

$$\rho \overline{u_i' u_j'} = 2\mu_t \frac{\partial u_i}{\partial x_j} - \left(\frac{2}{3}\right)\rho\kappa$$

μ_t = eddy viscosity, κ = turbelent kinetic energy.

$$Turbulent\ Kinetic\ Energy\ \kappa = \bar{\kappa} + \dot{\kappa}_i$$

$$\bar{\kappa} = \frac{\bar{u}_1^2 + \bar{u}_2^2 + \bar{u}_3^2}{2}$$

And

$\kappa_i = \frac{1}{2}\overline{u_i u_j} = Instataneous\ Kinetic\ Energy$ Now

subtracting equation (14) from equation (17) and doing some algebraic manipulation we will get, governing equation in terms of κ

$$\frac{\partial(\rho\kappa)}{\partial t} + \frac{\partial(\rho\kappa\, u_j)}{\partial x_i} = \frac{\partial}{\partial x_j}\left(\frac{\mu_t}{\sigma_k}\frac{\partial k}{\partial x_j}\right) + 2\mu_t \delta_{ij}\,\delta_{ij} - \rho\varepsilon \qquad (12)$$

Turbulent dissipation rate

$$\varepsilon = v_t \overline{\frac{\partial u_j'}{\partial x_j}\frac{\partial u_j'}{\partial x_j}} \quad v_t = \frac{\mu_t}{\rho} \quad , \mu_t = \frac{C_\mu\, \rho\kappa^2}{\epsilon}$$

$$\frac{\partial(\rho\varepsilon)}{\partial x} + \frac{\partial(\rho\varepsilon u_i)}{\partial x_i} = \frac{\partial}{\partial x_j}\left[\frac{\mu_t}{\sigma_\varepsilon}\frac{\partial\epsilon}{\partial x_j}\right] + C_{1\varepsilon}\frac{\varepsilon}{k}\,2\mu_t\,\delta_{ij}\delta_{ij} - C_{2\varepsilon}\,\rho\frac{\varepsilon^2}{\kappa} \quad [7]$$

Where δ_{ij} = Rate of Deformation, $C_{1\varepsilon} = 1.44$, $C_{2\varepsilon} = 1.92$ σ_k=1 σ_ϵ = 1.3 $C_\mu = o.09$

Solver Setting

for the solution of the problem, steady state, incompressible, water is used as the working Fluid.

Convergence Criteria: The solver is ANSYS CFX 15.30, it is possible to check convergence by continually tracking the imbalances that arise after each iteration. The imbalances discover the general flow variables preservation, and these are called the residuals. The residual is chosen as the 10 ^-4 order in this research. It is said that the solution converges when the residual reaches the specified tolerance and the head becomes constant with no iterations. Approximately 98 iterations are preserved as shown in Figure 3.17. The simulation is performed in a stable state. Following the specified no of iteration, as shown in Figure 3.18, the head developed by the pump is reached to a steady positive value of about 16 m.

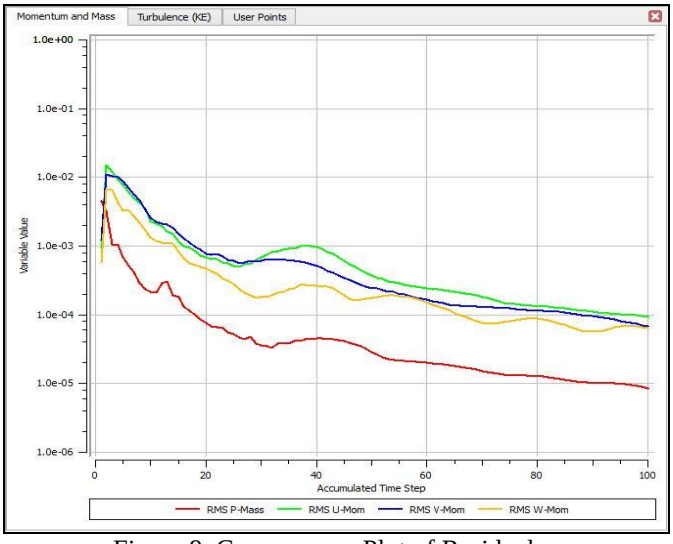

Figure 9. Convergence Plot of Residuals

IV. RESULT AND DISCUSSIONS

The pump generates different performance curve such as head, shaft power and complete effectiveness by varying the m range through the centrifugal pump.

(1

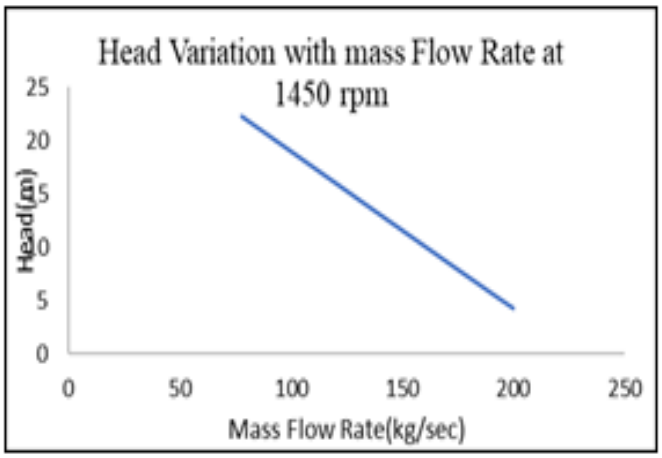

Figure 10. Head Developed by the Pump with Mass Flow Rate

The pump developed the maximum head of 22.28 m is 77.78 kg / sec and a minimum head of 200 kg / sec at the 4.3 m. The trend is in line with equation (9). The head variation with water mass flow rate follows the linear trend. The shaft power can be described by multiplying the angular velocity of the pump impeller radian / sec by the complete moment produced at the pump walls. The pump's peak power consumption at a weight flow rate of 100 kg / sec was discovered to be 19959 watts. The equation (5)[13] can define the shaft power consumed by the pump impeller.

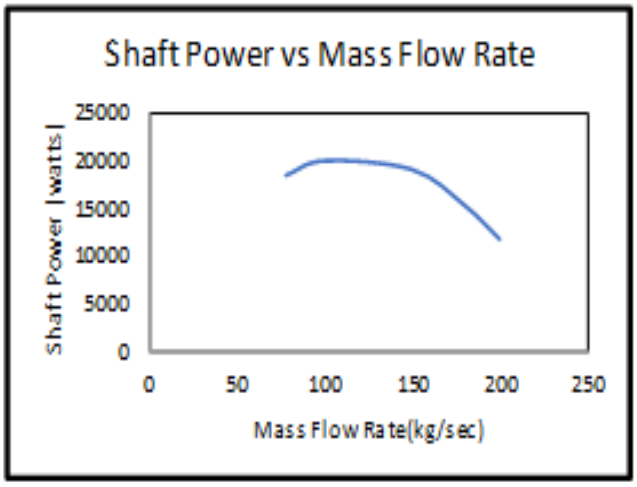

Figure 11. Shaft Power Consumed with Mass Flow Rate

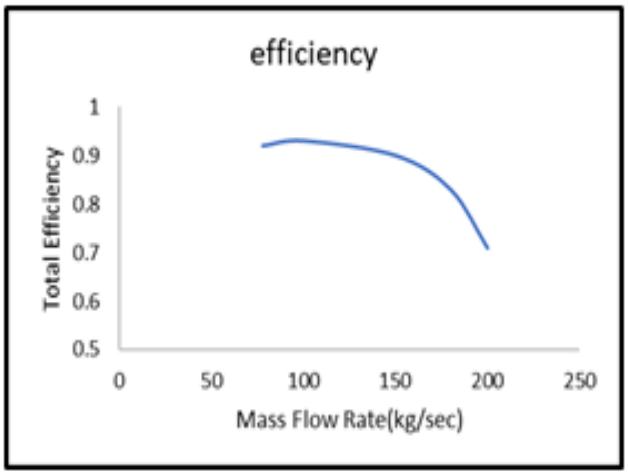

Figure 12. Total Efficiency of Centrifugal Pump Mass Flow Rate

The centrifugal pump's highest complete effectiveness is 93% and the minimum effectiveness is 71% at 100 and 200 kg / sec respectively. The equation can calculate the complete effectiveness (7). The trend is declining as the mass flow rate through the pump increases at a steady rate of 1450.

Table 3. Slip Factor Variation with outlet blade angle

S. No.	$\dot{m}(kg/sec)$	$\beta_2(°)$	σ
1	77.8	14.40	0.85
2	100	14.40	0.85
3	150	16.40	0.84
4	180	17.25	0.83
5	200	19.78	0.82

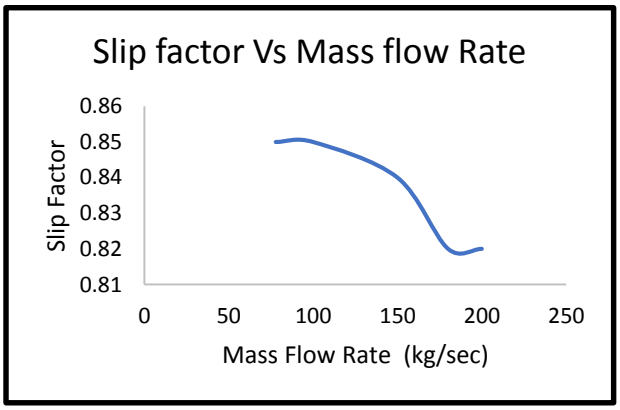

Figure 13. Slip Factor Variation with Mass Flow Rate

The slip factor reduces through the centrifugal with increased mass flow rate. The angle of the outlet blade is calculated at the impeller outlet by CFD simulation as shown in figure 4.4. Use the equation (11) to calculate the slip factor. It is possible to define total stress as static pressure plus dynamic pressure. The static pressure is the impeller's surface mass weighted average. Dynamic pressure is the stress induced by the fluid element's velocity.

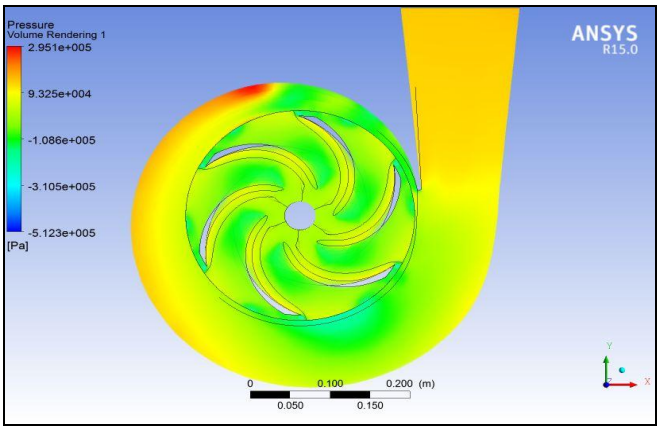

Figure 14. Total Pressure Contour

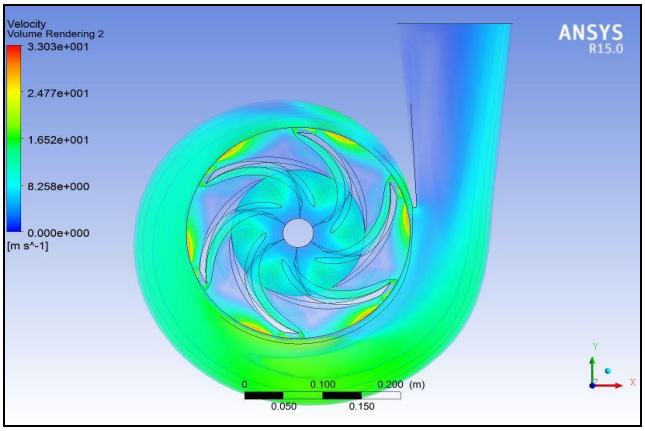

Figure 15. Velocity Contour

V. CONCLUSION

With the aid of ANSYS CFX 15.0, the current work explores the numerical efficiency of centrifugal pump and slip factor using CFD. As the mass flow rate rises through the centrifugal pump, shaft strength at linear declines, it is noted. The maximum head at 77.8 kg / sec discharge is 22.27 m. The shaft power consumed by the pump differs as the mass flow rate increased through the pump. The pump's highest power consumption is at a mass flow rate of 100 kg / sec in 19959.2 watts. The pump's total effectiveness differs nonlinear at a release of 77.8 kg / sec with a peak effectiveness of 92 percent. Mass Flow Rate has little impact on the outlet blade angle through the centrifugal pump. The calculated average slip factor has a value of 0.83 with a relative error of 5.06 percent to the empirical correlation of Wisner.

REFFERENCES

[1] B. Jafarzadeh, A. Hajari, M. M. Alishahi, and M. H. Akbari, "The flow simulation of a low-specific-speed high-speed centrifugal pump," *Appl. Math. Model.*, vol. 35, no. 1, pp. 242–249, 2011.

[2] J. M. Huang, K. W. Luo, C. F. Chen, C. P. Chiang, T. Y. Wu, and C. H. Chen, "Numerical investigations of slip phenomena in centrifugal compressor impellers," *Int. J. Turbo Jet Engines*, vol. 30, no. 1, pp. 123–132, 2013.

[3] X. Song, H. G. Wood, and D. Olsen, "Computational Fluid Dynamics (CFD) Study of the 4th Generation Prototype of a Continuous Flow Ventricular Assist Device (VAD)," *J. Biomech. Eng.*, vol. 126, no. 2, p. 180, 2004.

[4] C. and Y. Tu, J., Liu, *Computational fluid dynamics*. 2018.

[5] A. J. Stepanoff, "Cavitation Properties of Liquids," *J. Eng. Power*, vol. 86, no. 2, p. 195, 2012.

[6] Y. Fu *et al.*, "Numerical and Experimental Analysis of Flow Phenomena in a Centrifugal Pump Operating Under Low Flow Rates," *J. Fluids Eng.*, vol. 137, no. 1, p. 11102, 2014.

[7] S. . Som, *Introduction to fluid mechanics and fluid machines*. 2012.

[8] F. J. Wiesner, "A Review of Slip Factors for Centrifugal Impellers," *J. Eng. Gas Turbines Power*, vol. 89, no. 4, p. 558, 1967.

[9] W. Zhou, Z. Zhao, T. S. Lee, S. H. Winoto, and Z. Weidong, "Investigation of Flow Through Centrifugal Pump Impellers Using Computational Fluid Dynamics Computational fluid dynamics (CFD) analysis is being in- creasingly applied in the design of centrifugal pumps. With the," *Int. J. Rotating Mach.*, vol. 9, no. 1, pp. 49–61, 2003.

[10] J. A. Caridad and F. Kenyery, "Slip Factor for Centrifugal Impellers Under Single and Two-Phase Flow Conditions," *J. Fluids Eng.*, vol. 127, no. 2, p. 317, 2005.

[11] M. G. Khalafallah, H. A. Elsheshtawy, A. N. M. Ahmed, and A. I. Abd El-Rahman, "Flow simulation in radial pump impellers and evaluation of slip factor," *Proc. Inst. Mech. Eng. Part A J. Power Energy*, vol. 229, no. 8, pp. 1032–1041, 2015.

[12] H. Yousefi, Y. Noorollahi, M. Tahani, R. Fahimi, and S. Saremian, "Numerical simulation for obtaining optimal impeller's blade parameters of a centrifugal pump for high-viscosity fluid pumping," *Sustain. Energy Technol. Assessments*, vol. 34, no. August 2018, pp. 16–26, 2019.

[13] R. Stephens and J. Imberger, "Reservoir Destratification via Mechanical Mixers," *J. Hydraul. Eng.*, vol. 119, no. 4, pp. 438–457, 2006.

[14] J. A. A, S. E. A. Stephen, and R. S. D. S, "International conference on Recent Advances in Aerospace Engineering (ICRAAE-2017)," *IOP Conf. Ser. Mater. Sci. Eng.*, vol. 247, p. 11002, 2017.

[15] G. R. H. Abo Elyamin, M. A. Bassily, K. Y. Khalil, and M. S. Gomaa, "Effect of impeller blades number on the performance of a centrifugal pump," *Alexandria Eng. J.*, vol. 58, no. 1, pp. 39–48, 2019.

[16] M. Lorusso *et al.*, "Efficient CFD evaluation of the NPSH for centrifugal pumps," *Energy Procedia*, vol. 126, pp. 778–785, 2017.

[17] S. R. Patil, S. T. Chavan, N. S. Jadhav, and S. S. Vadgeri, "Effect of Volute Tongue Clearance Variation on Performance of Centrifugal Blower by Numerical and Experimental Analysis," *Mater. Today Proc.*, vol. 5, no. 2, pp. 3883–3894, 2018.

[18] S. Feng *et al.*, "Strengthening and toughening mechanisms in graphene-Al nanolaminated composite micro-pillars," *Acta Mater.*, vol. 125, pp. 98–108, 2017.

[19] M. Nataraj and R. Ragoth Singh, "Analyzing pump impeller for performance evaluation using RSM and CFD," *Desalin. Water Treat.*, vol. 52, no. February 2015, pp. 6822–6831, 2014.

[20] V. A. Grapsas, J. S. Anagnostopoulos, and D. E. Papantonis, "Hydrodynamic Design of Radial Flow Pump Impeller by Surface Parameterization," *1st Int. Conf. Exp. Model.*, no. July 2005, 2005.

[21] K. Subramanya, *Engineering hydraulics*. 2013.

[22] W.-G. Li, "Effects of Flow Rate and Viscosity on Slip Factor of Centrifugal Pump Handling Viscous Oils," *Int. J. Rotating Mach.*, vol. 2013, pp. 1–12, 2013.

[23] T. Engin, "Study of tip clearance effects in centrifugal fans with unshrouded impellers using computational fluid dynamics," *Proc. Inst. Mech. Eng. Part A J. Power Energy*, vol. 220, no. 6, pp. 599–610, 2006.

AUTHORS PROFILE

Mr. Jogendra Kumar completed M.Tech., Mechanical Engineering from MMMUT, Gorakhpur Uttar Pradesh, India in 2016. He is currently Pursuing Ph.D. in Department of Mechanical Engineering from MMMUT, Gorakhpur, Uttar Pradesh since 2018. He has published more than 3 research papers and it's available online. His main research work focuses on Machining, Optimisation, Design, FEM Simulation and Computational Intelligence based education. He has 2 years of teaching experience.

Mr. Maksudan Paswan pursed M.Tech., Mechanical Engineering from MMMUT, Gorakhpur Uttar Pradesh, India in 2017. He has published more than 2 research papers. His main research work focuses on Design, FEM Simulation and Computational Intelligence based education.

